Numerical Investigation of MHD Casson Nanofluid Blood Flow with Thermal Radiation in a Dilated Stenotic Artery Using Alumina and Ferric Oxide Nanoparticles

Abstract

This study investigates the numerical simulation of nanoparticle-enhanced non-Newtonian blood flow with internal heat generation in a dilated stenotic artery using the Casson fluid framework and analyzes the effects of different parameters on flow characteristics. The research is motivated by the need to understand the joined effects of nanoparticles, magnetic fields, and thermal radiation in stenosed arteries a topic with direct implications for targeted drug delivery and hyperthermia treatment in cardiovascular diseases.

The governing mathematical model is formulated applying the Casson fluid framework and modified to an ordinary differential equations in system form and numerically solved with the application of bvp4c solver in Maple. Graphical and tabular illustrations are used to examine key flow characteristics including velocity and temperature profiles, Nusselt number and coefficient of skin friction.

The outcomes display that velocity increases with rising curvature flow parameter, stenosis height, and nanoparticle volume fraction, whereas it drops with increasing magnetic field parameter and Casson fluid parameter. Temperature increases with Casson fluid parameter, curvature parameter, stenosis height, and magnetic field strength, but decreases with nanoparticle volume fraction, Prandtl number, and thermal radiation parameter. A slight but noticeable variation is observed between alumina (Al_2O_3) and ferric oxide (Fe_3O_4) nanoparticles with respect to the volume-fraction parameter.

The study gives valuable understanding to the behavior of nanofluid fluid flow in stenosed arteries, which may guide the development of effective therapeutic and diagnostic techniques for cardiovascular diseases, particularly in selecting appropriate nanoparticles for targeted therapy. The numerical approach using bvp4c solver proves effective for analyzing complex hemodynamic phenomena.

Keywords: Casson Nanofluid; Thermal Radiation; Dilated Artery; Alumina; Ferric Oxide; Cardiovascular; Magnetohydrodynamic

2020 Mathematics Subject Classification: 76Z05; 76W05; 80A20; 92C35

1 Introduction

Nanoparticles are ultrafine materials, typically ranging from 1–100 nm in size, and are invisible to the naked eye without advanced electron microscopy. Their interaction with blood flow has attracted substantial attention due to their potential applications in targeted delivery of drugs, biomedical diagnostics, and the analysis of blood rheology. When introduced into the bloodstream, nanoparticles can significantly influence hemodynamic characteristics and thermal behavior, particularly in diseased vessels.

Ahmed and Nadeem (2016) demonstrated that incorporating nanoparticles such as copper, titanium dioxide, and aluminum oxide can alter the hemodynamic properties of blood flowing through stenosed arteries while exhibiting antimicrobial effects that may aid prevent infections in diseased vessels. Similarly, Sarwar et al. (2022) investigated thermal enhancement in blood nanofluid flow through stenotic arteries using gold nanoparticles within a Sisko non-Newtonian fluid model. Their investigations indicated improved thermal performance and highlighted the potential of nanoparticles for localized drug delivery in regions of restricted blood flow.

Stenosis, defined as the constriction of an artery, is primarily caused by atherosclerotic plaque formation, inflammation, or hereditary disorders. It represents a significant cardiovascular risk factor due to its ability to restrict blood flow and increase the likelihood of severe complications such as ischemic stroke and myocardial infarction. Understanding the interaction between nanoparticles and stenosed arteries is therefore essential for advancing therapeutic and diagnostic strategies. In this context, alumina (Al_2O_3) and ferric oxide (Fe_3O_4) nanoparticles have gained particular attention due to their thermal, magnetic, and biocompatible properties, which can strongly influence flow behavior and arterial wall interactions.

Several recent works highlight the growing interest in employing nanoparticles for biomedical applications. Jerka et al. (2024) examined nanoparticle-mediated influences on endothelial cell transport, while Zuberi et al. (2024) investigated thermophoresis and Brownian motion in Casson nanofluid flows over nonlinear stretching surfaces. Their results provide deeper insights into nanoparticle-driven transport phenomena relevant to heat transfer and biomedical engineering.

Past studies have also explored the advantages of various nanoparticle materials. Shahzad et al. (2022), Karmakar et al. (2023), and Muhtamilselvan et al. (2023) focused on gold nanoparticles owing to their unique optical properties and imaging capabilities. Conversely, Gandhi et al. (2023) and Das et al. (2023) investigated alumina and iron oxide nanopar-

ticles for their magnetic responsiveness, enabling targeted delivery within stenotic regions. Titanium dioxide nanoparticles have also been used due to their biocompatibility and photocatalytic activity, offering therapeutic potential in vascular medicine.

Copper and alumina nanoparticles have shown distinct benefits in modulating physiological processes such as oxidative stress, inflammation, and endothelial dysfunction—key contributors to stenosis progression (Haris et al., 2024; Lin et al., 2024). Their tunable physicochemical properties permit precise targeting of arterial walls, enabling localized therapy while minimizing systemic side effects. However, challenges such as nanoparticle aggregation, altered effective viscosity, and deviations from Newtonian fluid behavior must also be considered.

The use of hybrid nanoparticles has expanded rapidly. Studies by Poonam et al. (2022), Khanduri et al. (2024), Jalili et al. (2023), and Manchi & Ponalagusamy (2022) examined the mutually reinforcing influence different nanofluid types such as silica iron oxide or silver gold hybrids to enhance imaging, cooling efficiency, or drug delivery capabilities in stenosed arteries. Other researchers have explored magneto-bio-hybrid nanofluids (Basha et al., 2022), thrombosis generation using magnetic fields (Hussain et al., 2023), and tri-hybrid nanofluids in Casson fluid models (Karmakar et al., 2023). These works collectively underscore the growing applicability of nanoparticle-enhanced fluids in treating vascular diseases.

More recent investigations include the effects of magnetic fields on heat transfer (Kabeel et al., 2015), magnetohydrodynamic hybrid nanofluid flow for drug delivery (Alghamdi et al., 2021), electromagnetic hybrid nano-blood pumping (Das et al., 2021), and sophisticated computational approaches such as machine-learning-assisted predictions of blood flow parameters in stenosed arteries (Li et al., 2024). Studies by Zuberi et al. (2024) and Dhange et al. (2025) further expanded the understanding of nanofluid behavior under complex arterial geometries and force-field interactions.

Motivated by these developments, the present study focuses on a Casson nanofluid model with water as the base-fluid and aluminum oxide and ferric oxide nanoparticles. The aim is to address critical gaps in existing research by examining the combined effects of nanoparticles, thermal radiation, magnetic field, and arterial dilation on blood flow and heat transfer in stenotic arteries. This work provides new insights that may guide the development of effective therapeutic and diagnostic techniques for cardiovascular diseases.

2 Formulation of the Problem

The geometry of this present problem can be expressed mathematically as Bhuvana et al. (2016):

$$R(x) = \begin{cases} R_0 - \frac{\delta}{2}\left[1 + \cos\frac{2\pi}{l_i}\left(\bar{x} - \beta_i - \frac{l_i}{2}\right)\right], & \beta_i \le \bar{x} \le \omega_i,\ i = 1, 2 \\ R_0, & \text{otherwise} \end{cases} \tag{1}$$

where $R(x)$ represents the radius of the artery in the stenosed part, R_0 represents the radius of the artery in the absence of stenosis, l_i is the irregular section length, ϕ is a constant, δ is critical height, which develops in two different locations $\bar{x} = \beta_1 + \frac{l_0}{2}$ and $\bar{x} = \beta_2 + \frac{l_0}{2}$.

The blood flow is modelled in arteries by Navier-Stokes equations for blood flow through a cylindrical artery Das et al. (2021) are:

$$\frac{\partial(ru)}{\partial x}+\frac{\partial(rv)}{\partial r}=0, \tag{2}$$

$$\rho_{\mathrm{nf}}\left(u\frac{\partial}{\partial x}+v\frac{\partial}{\partial r}\right)u=\mu_{\mathrm{nf}}\left(1+\frac{1}{\beta}\right)\left(\frac{\partial^2 u}{\partial r^2}+\frac{1}{r}\frac{\partial u}{\partial r}\right)-\sigma B(x)^2, \tag{3}$$

$$(\rho C_p)_{\mathrm{nf}}\left(u\frac{\partial}{\partial x}+v\frac{\partial}{\partial r}\right)T=k_{\mathrm{nf}}\left(\frac{\partial^2 T}{\partial r^2}+\frac{1}{r}\frac{\partial T}{\partial r}\right)-\frac{\partial q_r}{\partial r}. \tag{4}$$

From Rosseland's approximation, equation for the radiative flux q_r is defined as:

$$\frac{\partial q_r}{\partial r}=-\frac{4\sigma^*\partial T^4}{3k^*\partial r}, \tag{5}$$

where R, μ_{nf}, ρ_{nf}, k_{nf}, B, σ, C_p and T are the radius of the artery, dynamic blood viscosity, the blood density, Intensity of magnetization, electric conductivity of the blood, thermal conductivity, specific heat capacity and blood temperature in radial direction respectively. $\beta=\frac{\mu_b\sqrt{2\pi_k}}{\tau_y}$ represents the material parameter of Casson fluid, μ_b is the dynamic viscosity for plastic, τ_y the flow shear stress, $2\pi_k$ is critical value for the based product on the non-Newtonian flow.

The corresponding boundary conditions for the modelling equations are:

$$\begin{aligned} u=0,\quad v=0,\quad T=T_0,\quad &\text{at}\quad r=R(x)\\ \frac{\partial u}{\partial r}=0,\quad \frac{\partial T}{\partial r}=0,\quad &\text{at}\quad r=0 \end{aligned} \tag{6}$$

The thermal attributes of nanofluids as described by Haris et al., 2024 are employed in this research and are given by:

$$\begin{aligned} \frac{\rho_{\mathrm{nf}}}{\rho_f} &= \left((1-\phi)+\phi\frac{\rho_s}{\rho_f}\right),\\ \frac{\mu_{\mathrm{nf}}}{\mu_f} &= \frac{1}{(1-\phi)^{\frac{5}{2}}},\\ \frac{(\rho C_p)_{\mathrm{nf}}}{(\rho C_p)_f} &= \left((1-\phi)+\phi\frac{(\rho C_p)_{\mathrm{nf}}}{(\rho C_p)_f}\right),\\ \frac{k_{\mathrm{nf}}}{k_f} &= \frac{k_s+2k_{bf}-2\phi(k_{bf}-k_s)}{k_s+2k_{bf}+2\phi(k_{bf}-k_s)}. \end{aligned} \tag{7}$$

The coefficient of skin friction C_f and local Nusselt number Nu defined as:

$$C_f=\frac{\tau_w}{\frac{1}{2}\rho_f U_w^2},\quad \mathrm{Nu}=\frac{xq_w}{k_f(T_w-T_\infty)}. \tag{8}$$

The thermal flux q_w and drag force τ_w are given by:

$$q_w=-k_{\mathrm{nf}}\frac{\partial T}{\partial r}\bigg|_{r=R}.\qquad \tau_w=\mu_{\mathrm{nf}}\frac{\partial u}{\partial r}\bigg|_{r=R}, \tag{9}$$

Using dimensionless parameters, the skin friction and Nusselt number can be expressed as:

$$C_f = \frac{1}{T_1 \mathrm{Re}_x^{\frac{1}{2}}} F''(0), \quad \mathrm{Nu}_x = -\frac{k_{\mathrm{nf}}}{k_f} \mathrm{Rd}\theta'(0), \tag{10}$$

where $\mathrm{Re}_x^{\frac{1}{2}}$ is the local Reynolds number.

Table 1: The properties of thermo physical for base-fluid and nanofluids

Property	Base fluid (Blood)	Alumina (Al_2O_3)	Ferric Oxide (Fe_3O_4)
ρ (kg/m^3)	1063	3970	4000
k (W/(m K))	0.4920	40	2
C_p (J/(kg K))	3594	765	700
ξ (K^{-1})	18000	85000	–

3 Methodology

The intricacy of the governing equations warranted the utilization of an advanced numerical scheme, the module of bvp4c in Maple, since while dealing with complicated boundary value problems that involve non-linearities, stiff equations, or complex boundary conditions, conventional solvers struggle to produce accurate results efficiently. In such cases, the bvp4c solver shines by offering robust solutions with high accuracy and stability. The bvp4c solver's versatility enables it to address diverse problems across multiple domains, providing researchers and engineers with a robust tool for modeling and analyzing complex phenomena. Its significance stems from its capacity to resolve the inherent difficulties associated with complex boundary value problems, thereby enabling users to derive meaningful insights and make informed decisions across fields ranging from engineering and physics to biology and finance.

In the present problem, the nonlinear coupled ordinary differential equations, together with their associated boundary conditions, are solved numerically using the shooting technique implemented through the bvp4c solver—a built-in function in the computational software Maple. At this stage, the higher-order system of equations is transformed into a first-order system as follows:

$$\begin{array}{llll} F & = p_1, & F' = p_1' = p_2, & F'' = p_2' = p_3, \\ F''' & = p_3', & \theta = p_4, & \theta' = p_4' = p_5, \quad \theta'' = p_5'. \end{array} \tag{11}$$

The transformed equations are:

$$F''' = \frac{-2\xi F''' - T_1 T_2 (F F''' - F'^2 - M F')}{(1 + 2\xi\eta)}, \tag{12}$$

$$\theta'' = \frac{-2\mathrm{Rd}\xi\theta' - T_3 T_4 \mathrm{Pr}(F\theta' - F'\theta)}{(1 + 2\xi\eta)}. \tag{13}$$

The bvp4c solver requires initial guesses, after which it iteratively refines the solution by adjusting step sizes until the desired precision is attained. The selection of appropriate initial

guesses and boundary layer thickness depends on the specific parameter values employed. For this problem, a tolerance of 1×10^{-6} is specified. A custom numerical code is developed for this purpose, and the resulting solutions are presented graphically.

4 Discussion of the Results

The numerical simulation of alumina and ferric oxide nanoparticles on non-Newtonian blood flow through a stenotic and post-stenotic artery with heat transfer via the bvp4c module in Maple has been considered in this present study. To facilitate analysis, the governing differential equations are first normalized and subsequently solved using the fourth-order collocation method implemented via the bvp4c module in Maple. This methodological approach yields velocity and temperature profiles, thereby elucidating the significance of relevant parameters within the biomedical context.

The numerical solution employs various thermo-physical properties of blood, alumina, and ferric oxide nanoparticles, as presented in Table 1. The numerical values of the physical parameters are taken within the following ranges:

$$0.001 \leq \phi \leq 0.2; \quad 0.1 \leq \gamma \leq 0.4; \quad 0.1 \leq M \leq 2.2; \quad 3.6 \leq \mathrm{Pr} \leq 6; \quad 0.1 \leq \mathrm{Rd} \leq 1.2.$$

The numerical framework incorporates parameter values that authentically represent both the physiological attributes of blood and nanoparticles and the coupled influences of magnetic fields and thermal radiation. Through this rigorous calibration, the simulations yield meaningful insights into stenotic artery blood flow dynamics, offering contributions to biomedical research and potential therapeutic applications. The selected parameter ranges therefore establish a realistic foundation for investigating fluid behavior in stenosed arteries, supporting deeper exploration of this critical physiological phenomenon.

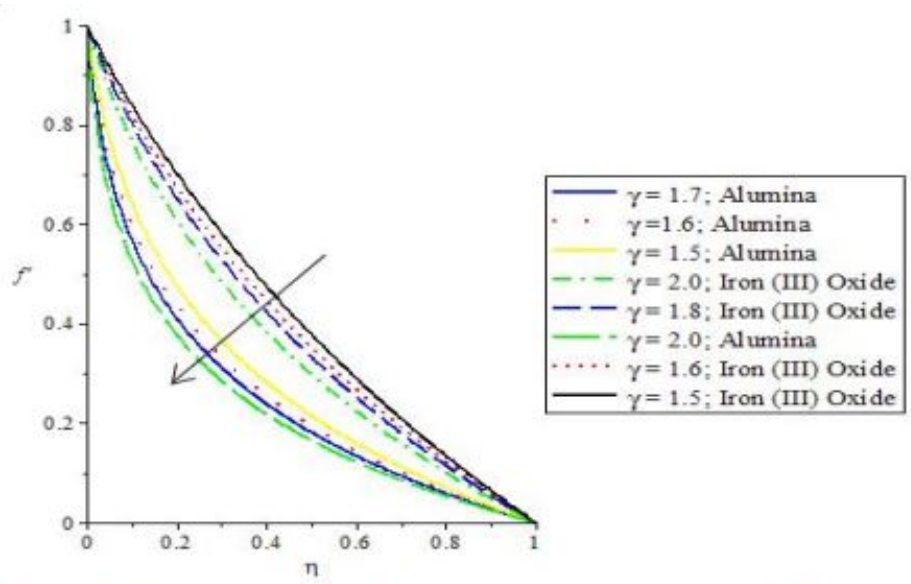

Figure 2: Velocity profiles for distinct values of Curvature flow parameter

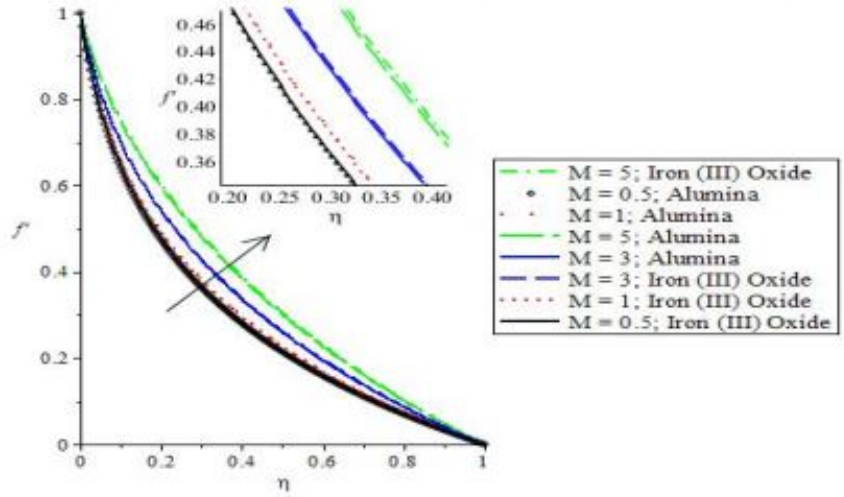

Figure 3: Velocity profiles for distinct values of magnetic parameter

Figure 1: Velocity profiles for different parameter values

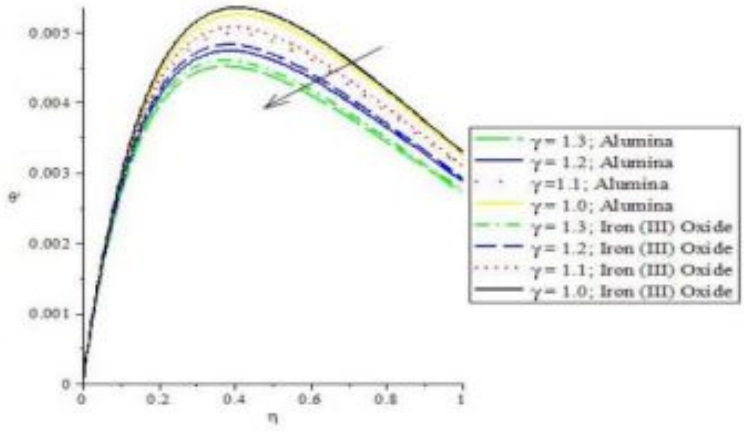

Figure 4: Temperature profiles for distinct values of Curvature flow parameter

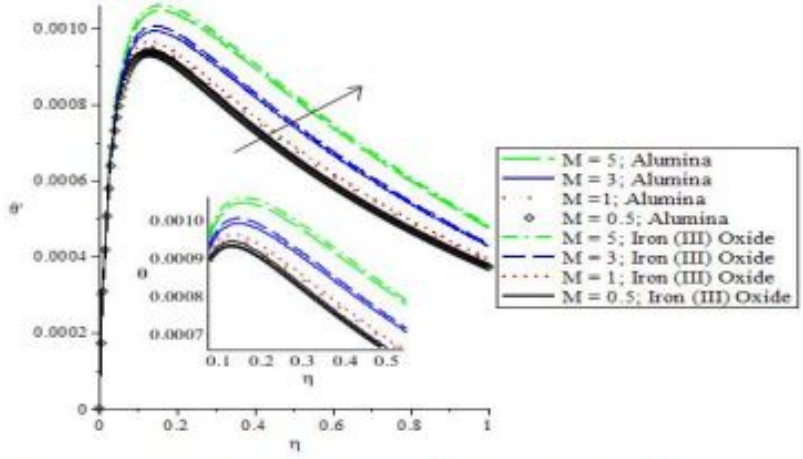

Figure 5: Temperature profiles for distinct values of Magnetic parameter

Figure 2: Velocity profiles for different parameter values

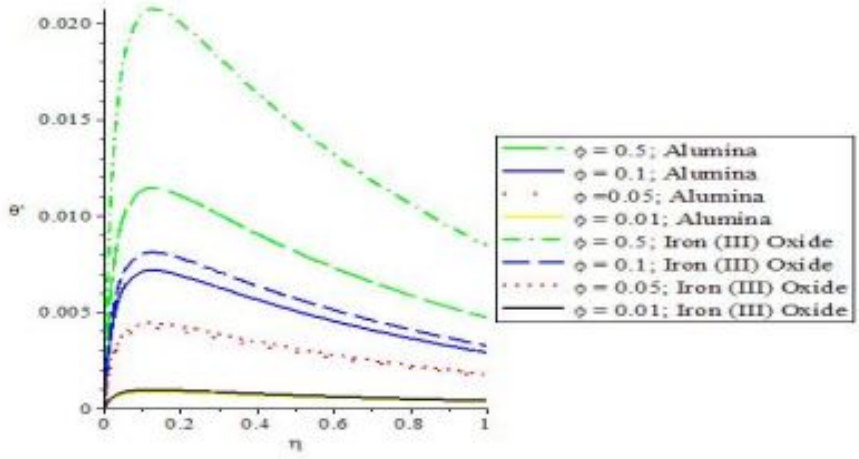

Figure 6: Temperature profiles for distinct values of Curvature flow parameter

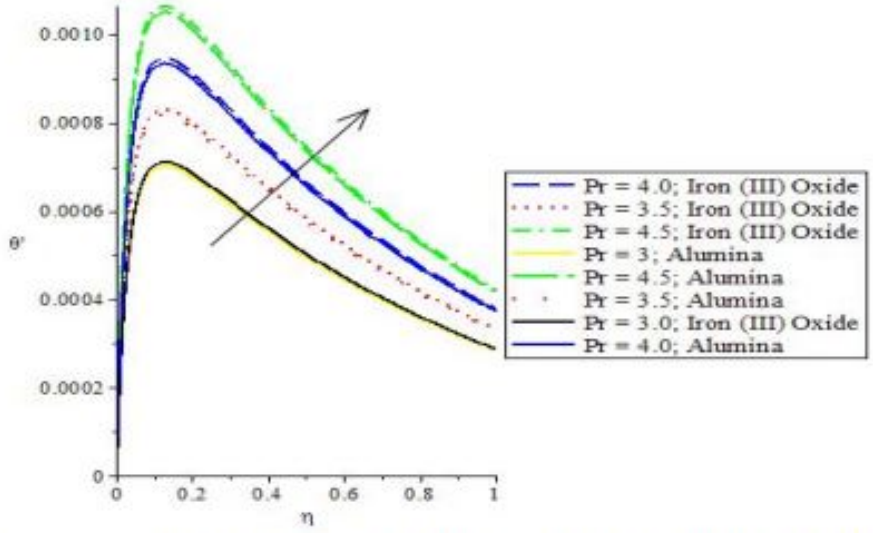

Figure 7: Temperature profiles for distinct values of Prandtl number

Figure 3: Temperature profiles for different parameter values

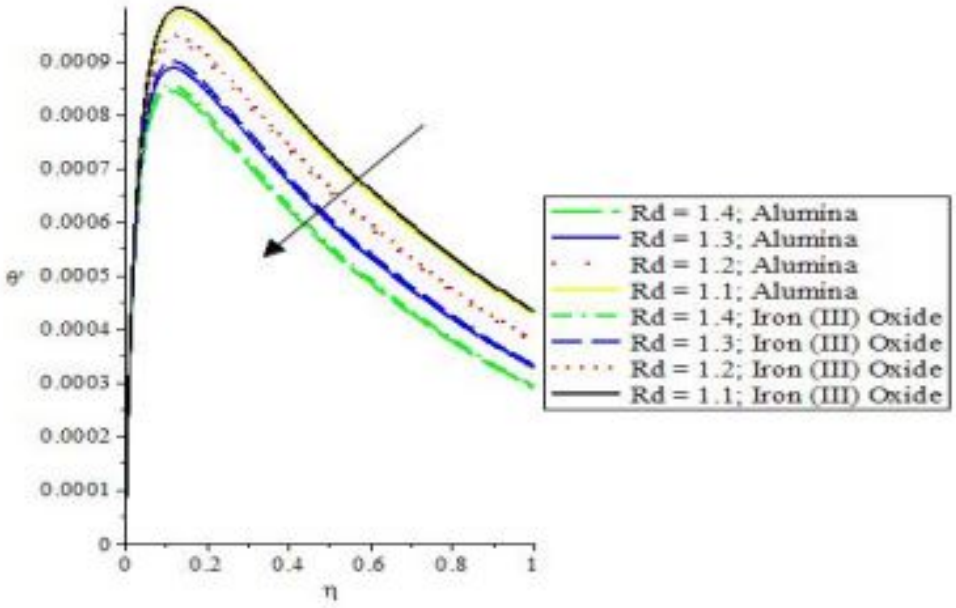

Figure 4: Temperature for values of Thermal radiation

Table 2: Comparison of Nusselt Number for Al_2O_3 nanoparticles with Haris et al. (2024) for Rd = 1

ϕ	Present Study	Haris et al. (2024)	% Error
0.10	2.43352	2.43366	0.0057
0.13	2.39458	2.39367	0.0380
0.16	2.34755	2.34680	0.0320
0.10	2.43361	2.43377	0.0066
0.13	2.76032	2.75763	0.0976
0.16	3.01784	3.01882	0.0324

Table 3: Comparison of Skin-Friction Coefficient for Al_2O_3 nanoparticles with Haris et al. (2024) for Rd = 1

ϕ	Present Study	Haris et al. (2024)	% Error
0.10	3.02572	3.02311	0.0862
0.13	3.00458	3.00865	0.1351
0.16	3.00117	3.00126	0.0030
0.10	3.02458	3.02700	0.0800
0.13	2.68034	2.68012	0.0081
0.16	2.35378	2.34269	0.4734

5 Conclusion

The present study investigated the numerical simulation of alumina and ferric oxide nanoparticles in a non-Newtonian Casson blood flow with internal heat generation through a dilated stenotic artery. Based on the obtained results, the following conclusions are drawn:

- **Temperature behaviour:** The temperature profile increases with rising Casson fluid parameter, curvature parameter, stenosis height, and magnetic field strength. Conversely, temperature decreases with increases in nanoparticle volume fraction, Prandtl number, and thermal radiation parameter.
- **Velocity behaviour (increase):** The velocity profile increases with higher curvature parameter, stenosis height, and nanoparticle volume fraction.
- **Velocity behaviour (decrease):** The velocity profile decreases as the magnetic field parameter and the Casson fluid parameter increase.
- **Nanoparticle comparison:** Alumina nanoparticles show a stronger response to changes in the volume fraction parameter compared to ferric oxide. However, both nanoparticles exhibit no significant differences in other parameter variations.

Acknowledgments

The authors would like to thank the reviewers for their constructive comments and suggestions that helped the improvement of this manuscript.

References

[1] A. Ahmed and S. Nadeem, The study of (Cu, TiO_2, Al_2O_3) nanoparticles as antimicrobials of blood flow through diseased arteries, *J. Mol. Liq.* 216 615-623, 2016.

[2] R. Manchi and R. Ponalagusamy, Modeling of pulsatile EMHD flow of Au-blood in an inclined porous tapered atherosclerotic vessel under periodic body acceleration, *Arch. Appl. Mech.* 91 (7) 3421-3447, 2021.

[3] L. Sarwar, A. Hussain, U. Fernandez-Gamiz, S. Akbar, A. Rehman and E. S. M. TagElDin, Thermal enhancement in blood nanofluid flow through stenotic arteries using gold nanoparticles within a Sisko non-Newtonian fluid model, *J. Therm. Anal. Calorim.* 147 123-135, 2022.

[4] D. Jerka, K. Bonowicz, K. Piekarska, S. Golyer, U. S. Derici and O. A. Hindy, Unraveling endothelial cell migration: insights into fundamental forces, inflammation, biomaterial applications, and tissue regeneration strategies, *ACS Appl. Bio Mater.* 7 (4) 2054-2069, 2024.

[5] H. A. Zuberi, M. Lal, S. Verma and N. A. Zainal, Computational investigation of Brownian motion and thermophoresis effect on blood-based Casson nanofluid on a non-linearly stretching sheet, *J. Adv. Res. Numer. Heat Transfer* 18 (1) 49-67, 2024.

[6] S. M. Mousavi, A. A. R. Darzi, O. Ali Akbari, D. Toghraie and A. Marzban, Numerical study of biomagnetic fluid flow in a duct with a constriction affected by a magnetic field, *J. Magn. Magn. Mater.* 473 42-50, 2019.

[7] D. F. Jamil, R. Roslan, M. Abdulhamed, N. Che-Him, S. Sufahani and M. Mohamad, Unsteady blood flow with nanoparticles through stenosed arteries in the presence of periodic body acceleration, *J. Phys.: Conf. Ser.* 995 012032, 2018.

[8] B. Vasu, A. Dubey, O. A. Beg and R. S. R. Gorla, Micropolar pulsatile blood flow conveying nanoparticles in a stenosed tapered artery: non-Newtonian pharmacodynamic simulation, *Comput. Biol. Med.* 126 104025, 2020.

[9] P. Karmakar and S. Das, Electro-blood circulation fusing gold and alumina nanoparticles in a diverging fatty artery, *BioNanoScience* 13 (2) 541-563, 2023.

[10] F. Shahzad, W. Jamshed, F. Aslam, R. Bashir, E. S. M. TagElDin and H. A. E. W. Khalifa, MHD pulsatile flow of blood-based silver and gold nanoparticles between two concentric cylinders, *Symmetry* 14 (11) 2254, 2022.

[11] M. Muhtamilselvan and Y. Gifteena Hingis, Flow characteristics of gold nanoparticles and microorganisms in a multistenotic artery treated with a catheter, *Aust. J. Mech. Eng.* 21 (1) 1-16, 2023.

[12] R. Gandhi, B. Sharma, Q. M. Al-Mdallal and H. Mittal, Entropy generation and shape effects analysis of hybrid nanoparticles (Cu-Al_2O_3/blood) mediated blood flow through a time-variant multistenotic artery, *Int. J. Thermofluids* 18 100336, 2023.

[13] S. Das, P. Karmakar and A. Ali, Simulation for bloodstream conveying bi-nanoparticles in an endoscopic canal with blood clot under intense electromagnetic force, *Wave Random Complex* 33 (1) 1-38, 2023.

[14] B. K. Sharma, U. Khanduri, N. K. Mishra, I. Albajjan and L. M. Perez, Entropy generation optimization for the electroosmotic MHD fluid flow over the curved stenosis artery in the presence of thrombosis, *Sci. Rep.* 13 (1) 15441, 2023.

[15] Y. Lin, R. Lin, H. B. Lin and S. Shen, Nanomedicine-based drug delivery strategies for the treatment of atherosclerosis, *Med. Drug Discov.* 22 100189, 2024.

[16] Poonam and B. K. Sharma, Mathematical analysis of hybrid nanoparticles (Au-Al_2O_3) on MHD blood flow through a curved artery with stenosis and aneurysm using hematocrit-dependent viscosity, In: *Nonlinear Dynamics and Applications*, Cham: Springer, 407-419, 2022.

[17] U. Khanduri and B. Sharma, Mathematical analysis of hall effect and hematocrit dependent viscosity on Au/GO blood hybrid nanofluid flow through a stenosed catheterized artery with thrombosis, In: *International Workshop of Mathematical Modelling, Applied Analysis and Computation*, Springer 17 121-137, 2024.

[18] P. Jalili, A. Sadeghi Ghahare, B. Jalili and D. Domiri Ganji, Analytical and numerical investigation of thermal distribution for hybrid nanofluid through an oblique artery with mild stenosis, *SN Appl. Sci.* 5 (4) 95, 2023.

[19] R. Manchi and R. Ponalagusamy, Pulsatile flow of EMHD micropolar hybrid nanofluid in a porous bifurcated artery with an overlapping stenosis in the presence of body acceleration and joule heating, *Braz. J. Phys.* 52 (2) 52, 2022.

[20] H. T. Basha, K. Rajagopal, N. A. Ahammad, S. Sathish and S. R. Gunakala, Finite difference computation of Au Cu/magneto-bio-hybrid nanofluid flow in an inclined uneven stenosis artery, *Complexity* 2022 1-18, 2022.

[21] A. Hussain, M. N. R. Dar, W. K. Cheema, Y. Han and R. Kanwal, Clinical symbiosis of hybrid nanoparticles and induced magnetic field on heat and mass transfer in multiple stenosed artery with erratic thrombosis, *Sci. Rep.* 13 (1) 15588, 2023.

[22] P. Karmakar and S. Das, Modeling non-Newtonian magnetized blood circulation with tri-nanoadditives in a charged artery, *J. Comput. Sci.* 70 102031, 2023.

[23] S. Das, B. Barman, R. Jana and O. Makinde, Hall and ion slip currents impact on electromagnetic blood flow conveying hybrid nanoparticles through an endoscope with peristaltic waves, *BioNanoScience* 11 (3) 770-792, 2021.

[24] M. Arif, L. Di Persio, P. Kumam, W. Watthavu and A. Akgul, Heat transfer analysis of fractional model of couple stress Casson tri-hybrid nanofluid using dissimilar shape nanoparticles in blood with biomedical applications, *Sci. Rep.* 13 (1) 4596, 2023.

[25] T. Nazar and M. Shabbir, Irreversibility analysis in the ternary nanofluid flow through an inclined artery via Caputo-Fabrizio fractional derivatives, *Results Phys.* 53 106992, 2023.

[26] A. Kabeel, E. M. El-Said and S. Dafea, A review of magnetic field effects on flow and heat transfer in liquids: present status and future potential for studies and applications, *Renew. Sustain. Energy Rev.* 45 830-837, 2015.

[27] W. Alghamdi, A. Alsubie, P. Kumam, A. Saeed and T. Gul, MHD hybrid nanofluid flow comprising the medication through a blood artery, *Sci. Rep.* 11 (1) 11621, 2021.

[28] Y. Li, D. Wan, D. Hu and C. Li, A novel approach for estimating blood flow dynamics factors of eccentric stenotic arteries based on ML, *Eng. Anal. Bound. Elem.* 163 175-185, 2024.

[29] P. G. Geredeli, H. Kunwar and H. Lee, Partitioning method for the finite element approximation of a 3D fluid-2D plate interaction system, *Numer. Methods Partial Differ. Equ.* 40 (6) e23132, 2024.

[30] H. A. Zuberi, M. Lal, S. Deo, A. Saxena, O. A. Beg, S. Kuharat et al., Computational hemodynamics of Sisko blood doped with gold and silver nanoparticles in a stenosed artery with porous walls, *Numer. Heat Transf. A: Appl.* (in press), 2024.

[31] H. A. Zuberi, M. Lal, A. Singh, N. A. Zainal and A. J. Chamkha, Numerical simulation of blood flow dynamics in a stenosed artery enhanced by copper and alumina nanoparticles, *Comp. Model. Eng. Sci.* 139 (2) 123-145, 2024.

[32] R. V. Bhuvana, K. P. Maruthi and C. Umadevi, A mathematical model for micropolar fluid flow through an artery with the effect of stenosis and post stenotic dilatation, *Appl. Appl. Math.* 11 680-692, 2016.

[33] M. Padma Devi, S. Srinivas and K. Vajravelu, Entropy generation in two-immiscible MHD flow of pulsating Casson fluid in a vertical porous space with Slip effects, *Journal of Thermal Analysis and Calorimetry* 149 7449-7468, 2024.

[34] M. Padma Devi, M. Ankamma Rao, B. Krishnaveni, V. Srinivasulu, A. Sombabu and G. V. Ramana Reddy, Effect of Melting Heat and Activation Energy on MHD Williamson Fluid Flow Over Parabolic and Plane Surfaces: A Numerical Approach, *Malaysian Journal of Mathematical Sci.* 3(19) 811-835, 2025 [DOI: 10.47836/mjms.19.3.03]

[35] M. Padma Devi and S. Srinivas, Heat transfer effects on the oscillatory MHD flow in a porous channel with two immiscible fluids, *Nonlinear Analysis: Modelling and Control* 3(28) 393-411, 2023 [DOI: 10.15388/namc.2023.28.31503]

[36] M. Ankamma Rao, E. K. Jaradat, M. P. Devi, P. B. Dhandapani, R. M. Nalule and M. Al-Hmoud, Modeling COVID-19 pneumonia and COVID-associated pulmonary aspergillosis: sensitivity analysis and optimal control, *BMC Infectious Diseases* 25:1192, 2025 [DOI: 10.1186/s12879-025-11606-x]